CONFERENCE PAPER

Optimizing proton exchange membrane water electrolyzers for enhanced green hydrogen production: a computational fluid dynamics approach

Amina Saidi[1] · Nihel Chekir[1]

Abstract

The performance of electrolyzers is profoundly influenced by pressure drops and water velocity within the flow channel. Higher pressure drops result in reduced water flow to the reacting location, consequently slowing down the electrochemical reaction rate and hydrogen release. To enhance overall performance, various types of flow channels were evaluated.

In this study, serpentine flow channels, commonly used in proton exchange membrane (PEM) water electrolyzer, were examined to assess their impact on their performance. Utilizing the fuel cell and electrolyzer module in ANSYS Fluent, 3D computational fluid dynamics (CFD) simulations were conducted. The analysis focused on elucidating the relationship between flow channel design and the concentration of oxygen and hydrogen. This article presents an innovative approach based on the development and assessment of a CFD model for simulating PEM water electrolyzers utilized in hydrogen production. The model's accuracy is validated through comparison with existing experimental data, with particular emphasis on assessing the effectiveness of the SIMPLE and COUPLED schemes in accurately capturing electrolysis processes.

The findings revealed that serpentine flow channels exhibited the highest oxygen and hydrogen concentrations within the voltage range of 1.5–2 V. Under steady conditions, the maximum hydrogen concentration in serpentine flow channels was determined to be 3.56×10^{-2} kmol/m^3. These results provide valuable insights into optimizing flow channel design for enhanced performance of PEM electrolyzers.

Abbreviations

IEA	International Energy Agency
PtX	Power-to-X
PEMWE	Proton exchange membrane water electrolyzers
AWE	Alkaline water electrolyzers
SOWE	Solid oxide water electrolyzers
PSA	Perfluoro sulfonic acid
HER	Hydrogen evolution reaction
OER	Oxygen evolution reaction
UDFs	User-defined functions
CFD	Computational fluid dynamic
MEA	Membrane electrode assembly
FEM	Finite element method
CAD	Computer-assisted design

Sub scripts

H_2	Hydrogen
H_2O	Water
O_2	Oxygen

Greek symbols

ρ	Density, kg/m^3
t	Time, s
u, v, and w	Velocities, m/s
μ	Dynamic viscosity, Ns/m^2
k	Heat transfer coefficient, W/mK
Φ	Dissipation function

✉ Nihel Chekir
nihel.chekir@univgb.tn

Amina Saidi
amina.saidi@enig.rnu.tn

1 Applied Thermodynamics Laboratory LR18ES33, National Engineering School of Gabes, University of Gabes, Gabes, Tunisia

Dimensionless quantities

E_{ocv}	Open circuit potential
η_{act}	Activation overpotential
η_{conc}	Concentration overpotential
η_{ohm}	Ohmic overpotential

Introduction

Today, scientists are looking at alternative methods of generating energy. This is because the primary source of energy (fossil fuel/commodities) has been shown by science to hurt the environment (Jouhara et al. 2020a). Once more, the cost of fossil fuels is unstable.

With renewable energies such as wind and solar projected to decrease in cost significantly according to the International Energy Agency (IEA) from 2022, there has been a surge in investment and research aimed at addressing their inherent variability. As global electricity demands continue to rise due to increased electrification across various sectors including transportation via electric vehicles, the challenge of storing renewable energy has gained unprecedented importance. To tackle this issue, several approaches are being explored. One strategy involves employing energy storage technologies, which store surplus electricity generated from renewables for later release onto the electrical grid during periods when renewable generation cannot fully satisfy demand. Alternatively, Power-to-X (PtX) techniques transform excessive renewable energy into alternate forms of energy carriers, such as gas, synthetic fuel, or hydrogen. These diverse solutions aim to ensure that renewable energy can consistently supply our growing needs while maintaining stability within the electrical grid.

Recent studies have looked at renewable energy as a possible replacement for fossil fuels because it is thought to be abundant, sustainable, and environmentally benign (Jouhara et al. 2020b). Countries all over the world are investing heavily in this industry.

Currently, the cost of producing hydrogen from fossil fuels ranges from $0.7 to $1.6 per kilogram, and incorporating carbon capture increases this to about $1.2 to $2.0 per kilogram. Conversely, generating hydrogen using electricity from renewable sources through water electrolysis technology costs approximately $3.2–7.7 per kilogram. Therefore, the profitability and scale of hydrogen production will be crucial for advancing electrolysis technology based on renewable energy. The deployment of large electrolyzers is a key component in decarbonizing major industrial and transportation sectors, with current cell technology poised for significant expansion (Ni et al. 2023).

It continues to be difficult to store the energy produced by renewable sources. Renewable energy is erratic and sporadic, making storage of this energy essential. When demand is low, excess electricity generated by renewable sources can be used to split water to produce hydrogen. Electrolysis is useful for energy management because it may produce electricity when there is a high demand for energy by using stored hydrogen and an energy converter such as a fuel cell. Because hydrogen does not serve a purpose in its molecular structure, several research initiatives are currently being supported in this gray region (Ijaodola et al. 2019). Hydrogen production requires an energy input. A well-known method for producing hydrogen is steam reforming of natural gas. Hydrogen is regarded as one of the greatest vectors/carriers for storing renewable and intermittent energy from sources such as wind and solar, as well as off-peak energy, from the grid, aside from being produced from propane, gasoline, diesel, methanol, or ethanol by steam reforming (Wu et al. 2011). The process of steam reforming involves heating fossil fuel to temperatures between 700 °C and 1100 °C and combining it with steam in the form of water vapor. This apparatus is known as the reformer. To accelerate the chemical reaction in the reformer, nickel is utilized as a catalyst. Low-quality hydrogen is created during steam reforming, and carbon-based molecules such as carbon monoxide are present in small amounts. The environment is still greatly impacted by the hydrogen produced by steam reforming, and this dependence on scarce fossil resources is not at all diminished.

Regarding water electrolysis, three primary types stand out: alkaline water electrolyzers (AWE), proton exchange membrane water electrolyzers (PEMWE), and solid oxide water electrolyzers (SOWE). Of these, PEMWE holds significant promise owing to numerous benefits compared with other options. Some of these advantages include lower corrosiveness, reversible functionality, efficient performance at reduced voltages, higher current densities, broader operational temperature ranges, greater intrinsic power output, capability to function under varying pressures, minimal ecological footprint, user-friendly operations, and streamlined design (Shiva Kumar and Himabindu 2019).

When discussing the optimization of proton exchange membrane (PEM) water electrolyzers for green hydrogen production, it is essential to situate this technology within the broader landscape of sustainable water management and clean energy production. While PEM water electrolyzers utilize electrochemical reactions to generate hydrogen, another emerging approach known as photocatalysis employs catalysts activated by light to drive hydrogen production (Baaloudj, et al. 2022). Both methods offer unique opportunities and challenges in achieving a sustainable hydrogen economy. A PEMWE utilizes a zero-pitch design to transport protons across the polymer membrane. Due to the quick response of proton movement on the membrane to changes in power, the PEMWE is well suited for integration with wind power and photovoltaic systems,

allowing for swift adjustments in load (Lu et al. 2023). Photocatalytic hydrogen production relies on semiconductors capable of absorbing sunlight and generating electron hole pairs, which subsequently participate in redox reactions to produce hydrogen. Although photocatalysis offers some distinct advantages, including the potential use of abundant natural resources and the possibility of decentralized applications, it also faces challenges related to efficiency, scalability, and long term stability (Kenfoud et al. 2022).

The proton exchange membrane water electrolyzer (PEMWE) originated in 1966 through development by General Electric Company. Its core components consist of a proton conducing membrane fabricated using perfluorosulfonic acid (PFSA), along with catalyst layers or electrocatalysts, gas diffusion layers, and bipolar plates (Grigoriev et al. 2020). Furthermore, a major drawback is the utilization of costly perfluorinated membranes and noble metal catalysts in the production of PEM electrolyzers. While it is possible to modify the components of the electrolyzer to enhance its performance, adjustments can certainly be made to the operating parameters. These parameters include the operating temperature of the PEMWE, water flow rate, bolt torque, cell voltage, and pressure, which must be carefully varied and optimized (Ozdemir et al. 2024).

In a proton exchange membrane water electrolyzer (PEMWE), water undergoes separation into hydrogen and oxygen at the cathode and anode electrodes, respectively, through the hydrogen evolution reaction (HER) and oxygen evolution reaction (OER). The anode decomposes water into oxygen, protons, and electrons, with the protons passing through the PEM to the cathode. At the cathode, the protons react with electrons to produce hydrogen gas. The voltage required to split water into hydrogen and oxygen depends on whether the reaction is reversible or irreversible. The reversible voltage is 1.23 V, while the thermoneutral voltage is 1.48 V. However, practical electrolyzers experience higher voltages due to irreversible losses called overpotentials. These overpotentials are caused by kinetic factors and are mainly categorized into activation, ohmic, and mass transport overpotentials. Therefore, the actual cell voltage is the sum of the thermoneutral voltage and overpotential (Carmo et al. 2013).

Hydrogen can be produced by electrochemically separating water into hydrogen and oxygen. Water electrolysis is the procedure, as demonstrated by Eq. (1)

$$H_2O \ + \ electricity \rightarrow H_2 \frac{1}{2} + O_2 \tag{1}$$
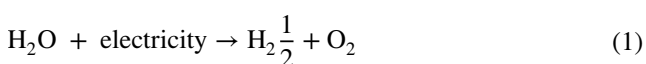
The chemical reactions employed in PEM electrolysis can be illustrated as:

For the anode

$$H_2O \rightarrow \frac{1}{2}O_2 + 2H^+ + 2e^- \tag{2}$$

For the cathode:

$$2H^+ + 2e^- \rightarrow H_2 \tag{3}$$
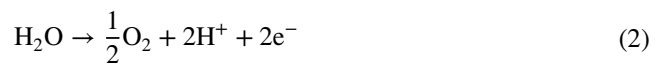
According to the principles of PEMWE technology, the catalyst layer is identified as the central location for energy conversion via electrochemical reactions. It remains essential to advance the production of cost-effective, high-performing catalysts to facilitate the widespread use of PEMWE technology (Wang and Feng 2023). Understanding the principles of PEMWE technology reveals that the catalyst layer plays a key role in converting energy through electrochemical reactions. Enhancing the activity of anode electrocatalysts is crucial for sustaining high performance in hydrogen production.

Modeling of 3D PEM electrolyzer

Modeling methodology

The PEM electrolyzer is selected as the preferred type of electrolyzer because it shares similarities with fuel cells and can achieve similar results using the same methods. Therefore, knowledge and experience gained from working with the PEM electrolyzer can directly benefit potential future applications of fuel cells. The modeling methodology involves various physical phenomena such as multiphase flow, turbulence, heat and mass transfer, charge transfer, and species transfer. One of the main objectives of the methodology is to avoid using user-defined functions (UDFs) and instead focus on utilizing the software's provided tools to simplify the modeling process as much as possible. This approach aims to make future simulations on the same subject easier to conduct. The CFD simulation assumes that the flow is incompressible and laminar. It also assumes that ideal gas mixtures are used as reactants. The electrolyzer cell's components and layers are made of uniform materials with consistent conductance properties, and there is no penetration of liquid water through the membrane.

Computational fluid dynamics involve the solution of numerical solver algorithms for the governing equations within a subdivided, or meshed, computational domain, also known as the finite volume method. As described by Versteeg and Malalasekera (Sousa et al. 2020), the algorithm can be broadly characterized in three stages: firstly, the governing equations are integrated over the finite control volumes of the computational domain. Secondly, the integral equations are discretized and converted into a system of algebraic equations. Finally, in the third stage, the equations are solved using an iterative method.

Governing equations

The governing equations, commonly recognized as Navier–Stokes equations, encompass principles for mass conservation, continuity, momentum in all Cartesian directions, and energy balance. Multiple representations exist for these equations, including integral and partial derivative forms. By Versteeg and Malalasekera (Sousa et al. 2020), the equations are demonstrated below in their partial derivative form:

For the continuity equation:

$$\frac{\partial \rho}{\partial t} \nabla \cdot (\rho \cdot u) = S_m \tag{4}$$

For x-momentum:

$$\frac{\partial(\rho \cdot u)}{\partial t} + \nabla \cdot (\rho \cdot v \cdot u) + \frac{\partial \rho}{\partial y} - \nabla(\mu \cdot \Delta u) = S_{Mx} \tag{5}$$

For y-momentum:

$$\frac{\partial(\rho.v)}{\partial t} + \nabla \cdot (\rho \cdot v \cdot u) + \frac{\partial \rho}{\partial t} - \nabla(\mu \cdot \Delta u) = S_{My} \tag{6}$$

For z-momentum:

$$\frac{\partial(\rho \cdot w)}{\partial t} + \nabla \cdot (\rho \cdot w \cdot u) + \frac{\partial \rho}{\partial z} - \nabla(\mu \cdot \Delta u) = S_{Mz} \tag{7}$$

the energy equation:

$$\frac{\partial(\rho \cdot i)}{\partial t} + \nabla \cdot (\rho \cdot i \cdot u) + p \cdot \nabla u - \nabla(k \cdot \Delta T) = \Phi + S_i \tag{8}$$

where

ρ: density (kg/m^3)
t: time (s)
u, v, and w: velocities (m/s)
μ: dynamic viscosity (Ns/m^2)
k: heat transfer coefficient (W/mK)
Φ: dissipation function
S_{Mi}, S_i: source terms

To represent how a cell performs on the basis of its voltage–current relationship, the total voltage applied to the cell from an electrical source is divided into different components and is equal to the combined total of individual overpotentials (Ma et al. 2021).

$$V = E_{ocv} + \eta_{act} + \eta_{conc} + \eta_{ohm} \tag{9}$$

where

E_{ocv}: open circuit potential
η_{act}: activation overpotential.
η_{conc}: concentration overpotential.
η_{ohm}: ohmic overpotential.

Geometry description

PEMWE is made up of an anode [where the oxygen evolution reaction (OER) occurs] and a cathode [where the hydrogen evolution reaction (HER) takes place], separated by an acidic proton exchange membrane. The diagram in Fig. 1 illustrates how PEM electrolyzers work and the internal components involved. In most cell designs, the electrodes are directly connected to the proton exchange membrane. This assembly, known as the membrane electrode assembly (MEA), is a crucial part of a PEM cell. Current collectors, also referred to as gas diffusion layers (GDL), are located on both sides of the MEA and allow water and product gases to pass through, enabling the flow of electric current to and from the electrodes. The two half cells are enclosed by



Fig. 1 Schematic of PEMWE (Majasan et al. 2021)
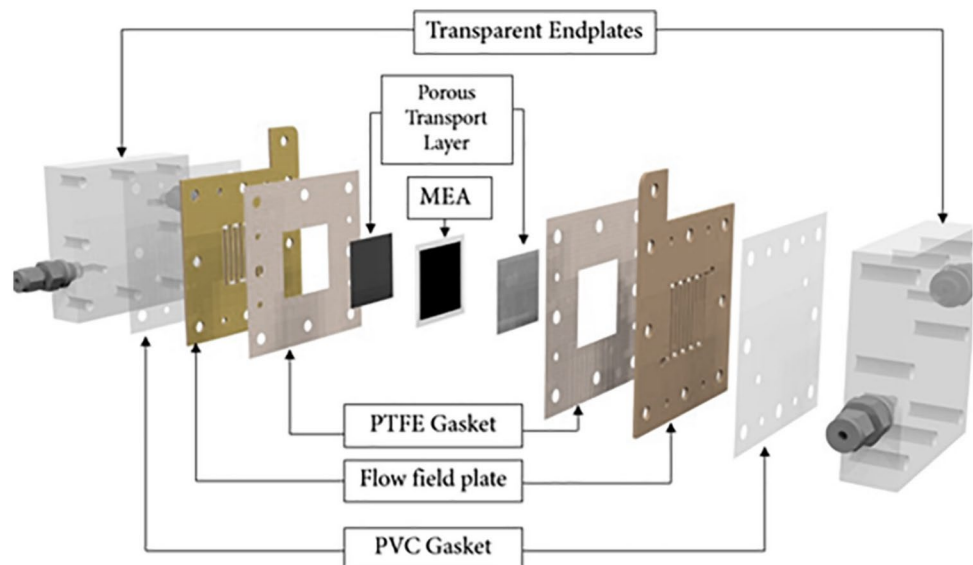
bipolar plates (BPP) that typically have flow fields. These plates are responsible for transporting the reactant water to the membrane–electrode interface and removing the product gases.

A 3D representation of a PEM electrolyzer's arrangement and its distinctive 9 layers are shown in Fig. 2. The design of the electrolyzer had to be made suitable for everyone so that all the other elements are constant. Just the flow channel needs to be modified to explore the impact of the flow channel on the performance of the electrolyzer. By doing this, the dimensions of the MEA, gasket, and current collectors were all maintained. The design of the gasket model is shown in Fig. 3 and the serpentine flow channel is given in Fig. 4. It had a land width of 1 mm, while the serpentine channel had a thickness of 0.2 mm. This was regarded as one of the ideal land widths for fuel cells with serpentine channels
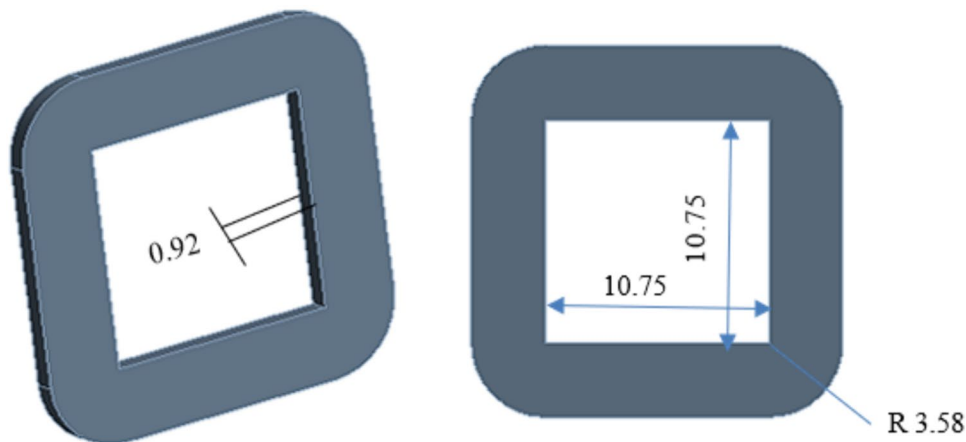
(Wilberforce et al. 2018). The current collector design is depicted in Fig. 5. The measurements were recorded in centimeters, and it was intended that the active area of the current collector correspond to the MEA, which for simulation purposes were set at roughly 17.90 mm^2. The design of the PEM water electrolysis was constructed on the basis of the measurements provided in the study by Wilberforce et al. (2018). The specific dimensions of the geometry area are outlined in Table 1.

The catalyst-coated Nafion membranes, which have three layers, are commonly employed in electrolyzers. It is necessary to create an MEA for the ANSYS fuel cell and electrolyzer module that has two gas diffusion layers, two catalyst layers, and one membrane layer.

Meshing

The precision and stability of the numerical computation are significantly influenced by the mesh quality. Node point distribution, smoothness, and skewness are characteristics connected to mesh quality. Checking the mesh quality is important regardless of the type of mesh employed in a domain.

Different quality criteria are assessed depending on the types of cells in the mesh (tetrahedral, hexahedral, polyhedral, etc.). With a maximum of 1,060,471 nodes and about 844,377 elements, structured meshing was taken into consideration for the construction of serpentine flow channels.

Solver setup and boundary conditions

Solver setup

All of the boundary conditions were kept consistent across all of the simulations to assess the impact of the flow channel on the electrolyzer's performance. To obtain converging findings, the mesh quality as previously described was set to skewness metrics and 800 iterations were completed. The energy balances between the anode and the cathode are
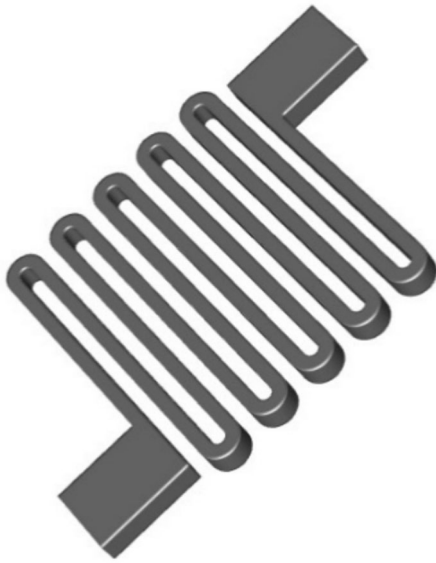

Fig. 2 3D design of PEM water electrolyzer

Fig. 3 3D gasket model for the design

Fig. 4 Serpentine flow channel

Fig. 5 Current collector

Table 1 PEM water electrolyzer dimensions

Element	Value
PEM length	17.90 mm
PEM height	3.83 mm
PEM width	17.90 mm
Membrane thickness	0.180 mm
Gas diffusion layers' thickness	0.184 mm
Serpentine flow channel width	12.30 mm
Serpentine flow channel height	0.98 mm

Table 2 Simulation parameters used in ANSYS Fuel Cell and Electrolyzer Module (Khatib et al. 2021)

Parameter	Unit	Anode	Cathode	Global
Reference current density	(A/m^2)	10.000	20	–
Reference concentration	(kmol/m^3)	1	1	–
Concentration exponent	–	0.5	1	–
Exchange coefficient (a)	–	2	2	–
Exchange coefficient (c)	–	2	2	–
Open voltage	V			1.19

considered during the ANSYS simulation of the "fuel cell and electrolyzer module." This energy balance depends on several variables, including the temperature, the boundary conditions, the species present (H_2, O_2, H_2O), and more.

The energy equation estimates the corresponding current density needed for the electrolyzer to produce the species, laminar flow within the channels, and membrane dynamics by determining the voltage level at the current collector. The energy equation was used as the conversion criteria in the simulation, with a tolerance of 10^{-6}.

Numerous researchers have investigated and used the serpentine flow channel design extensively, and it is regarded as the industry standard for flow design in most fuel cells. Because it supports the full utilization of the active surface and coverage of gas at acceptable pressure losses, many businesses choose this design as their primary flow plate design in the production of PEM fuel cells. The attributes and simulation parameters are presented in Table 2 (Khatib et al. 2021).

Once the model parameters for the cell were established, the components that were defined and named when creating the geometry were identified and assigned to each zone on both the anode and cathode sides, as well as the tab surfaces. The characteristics of these zones are detailed in Table 3.

After selecting the appropriately named components in the geometry, such as the tab surfaces on both the anode and cathode sides, the electrochemistry model was applied to automatically update the cell zones and walls of the electrolyzer. Additionally, the energy equation and species transport equation were activated automatically. The material properties of the uniform components and layers are detailed in Table 4.

Table 3 Characteristics of the porous zones in the PEM water electrolyzer

Component	Parameter unit	Anode	Cathode
Gas diffusion layer	Porosity	0.5	0.5
	Absolute permeability (m^2)	1.00×10^{-12}	1.00×10^{-12}
Catalyst layer	Porosity	0.2	0.2
	Absolute permeability (m^2)	4.90×10^{-12}	2.00×10^{-12}
	Surface volume ratio (1/m)	20,000	20,000

Table 4 Material properties for the components of the PEM electrolyzer

	Thermal conductivity (W/mK)	Electrical conductivity (S/m)	Electrolyte conductivity (S/m)
Current collector	100	20,000	10^{-16}
Gas Diffusion Layer	10	20,000	10^{-16}
Catalyst layer	10	5000	4.5
Membrane	2	10^{-16}	11

Boundary conditions

The boundary conditions of the PEM water electrolyzer are presented in Table 5.

The simulations used the SIMPLE scheme for pressure–velocity coupling, and first order upwind schemes were chosen for all spatial discretization. Convergence criteria were set at 10^{-6} for the residuals of the governing equations. Volumetric transfer currents at the catalyst layers and volume integrated velocities at various components were monitored to check for convergence. Once convergence or near convergence was achieved, heat transfer in the electrolyzer was enabled by activating Joule heating and reaction heat from the electrochemistry model. The solver then continued iterating the solution until convergence was reached.

Another approach to pressure–velocity coupling is the COUPLED scheme, which allows users to modify the pseudo-transient global time step of steady-state flow. This is achieved through a parameter known as the time scale factor, which adjusts the automatically determined size of the pseudo-time step on the basis of the minimum fluid time scales of equations representing various physical aspects of fluid flow, such as convection and gravity. By scaling the global time step size using the time scale factor, convergence is often improved. In this study, the COUPLED scheme was utilized to compare pressure–velocity coupling methods in simulations of electrolyzers.

Results and discussions

Validation

According to literature sources, the primary approach for validating and assessing the accuracy of CFD simulations in modeling electrolyzers is by comparing polarization data. This involves comparing the polarization table derived from simulation results with actual measured data, as presented in Table 6.

After analyzing the polarization data, it can be inferred that the model delivers satisfactory performance in terms of accuracy. The main inconsistencies are observed at lower voltage levels, a trend that has been identified in various studies on the topic. The computational fluid dynamic (CFD) simulations showed satisfactory results with increasing voltage. Similar findings were reported in a study by Khatib et al. (2021) in which the simulated electrolyzer cell exhibited lower current density values at lower voltages compared with actual measurements. However, discrepancies were more pronounced at higher voltages in that study, unlike

Table 5 Boundary conditions

Interface	Type	Value	Thermal	Species H$_2$ O$_2$ H$_2$O
Anode inlet	Velocity inlet	1	360.65 K	0 0 1
Anode outlet	Pressure outlet	0	360.65 K	0 0 0
Cathode inlet	Velocity inlet	0	360.65 K	0 0 0
Cathode outlet	Pressure outlet	0	360.65 K	0 0 0
Anode current collector	Wall	1.3–1.8 V	360.65 K	N/A
Cathod current collector	Wall	0	360.65 K	N/A

Table 6 Polarization validation test

Experiment		Numerical			
Temperature, °C	Current density A/m^2	Current density A/m^2		Relative error, %	
	Voltage, V	Voltage, V		Voltage, V	
	2	2.5	2	2.5	2	2.5
30	0.18	0.38	0.1925	0.3957	6.9521	4.15556
50	0.22	0.52	0.2336873	0.5476	6.2215	5.3263

the simulation results in this paper. The variations between the current simulations and those conducted by Khatib et al. (2021) are likely due to differences in how the electrochemistry equations were implemented. While the previous study used self-written equations in UDFs, the current model relied on the software's built-in tools.

Many academics used CFD modeling methods in their research to create and improve bipolar flow plates. CFD, FEM, and many forms of programming methods are used by ANSYS, Inc., a company that creates engineering simulation software (often known as computer-aided engineering, or CAE). The five steps of any ANSYS project simulation include meshing, creating the geometry, setting up the simulation, conducting the calculations, and post-processing.

The total output hydrogen concentration flowing out of the cathode side for both pressure–velocity coupling schemes have been recorded in Table 7.

Results with the SIMPLE scheme

Contours of the concentration of hydrogen at the serpentine cathode channel for simulated voltage levels of (a) 1.5 V and (b) 2 V solved with the SIMPLE pressure–velocity coupling are depicted in Fig. 6. Those at the anode are shown in Fig. 7. Figure 8 depicts the concentration of hydrogen and oxygen at the membrane interfaces to the cathode and anode portions of the channel, respectively.

Results with the COUPLED scheme

In the COUPLED scheme, Fig. 9 displays the hydrogen concentration levels for two different voltages. Similarly, the levels of oxygen concentration on the anode side can be observed in Fig. 10, while the concentration of hydrogen at the cathode interface of the PEM cell membrane is depicted in Fig. 11.

Discussion

The concentration of hydrogen appears to be very similar in both the SIMPLE laminar and COUPLED turbulent simulations when compared.

One important finding confirmed by the results is that the cell's performance improves as its voltage is raised.
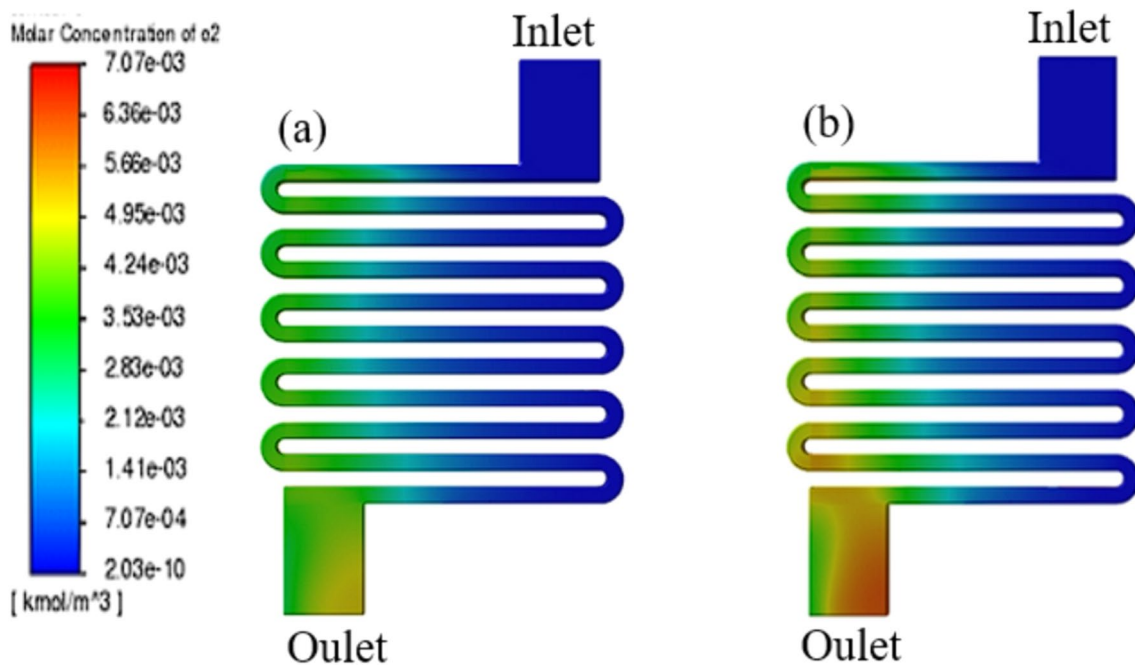
Table 7 Concentration (kmol/m^3) of hydrogen in the cathode side outlet for two voltages, from both schemes

| SIMPLE		COUPLED	
Voltage, V	Hydrogen concentration, kmol/m^3 (Cathode outlet)	Voltage, V	Hydrogen concentration, kmol/m^3 (Cathode outlet)
1.5	0.0304	1.5	0.0304
2	0.0305	2	0.0315
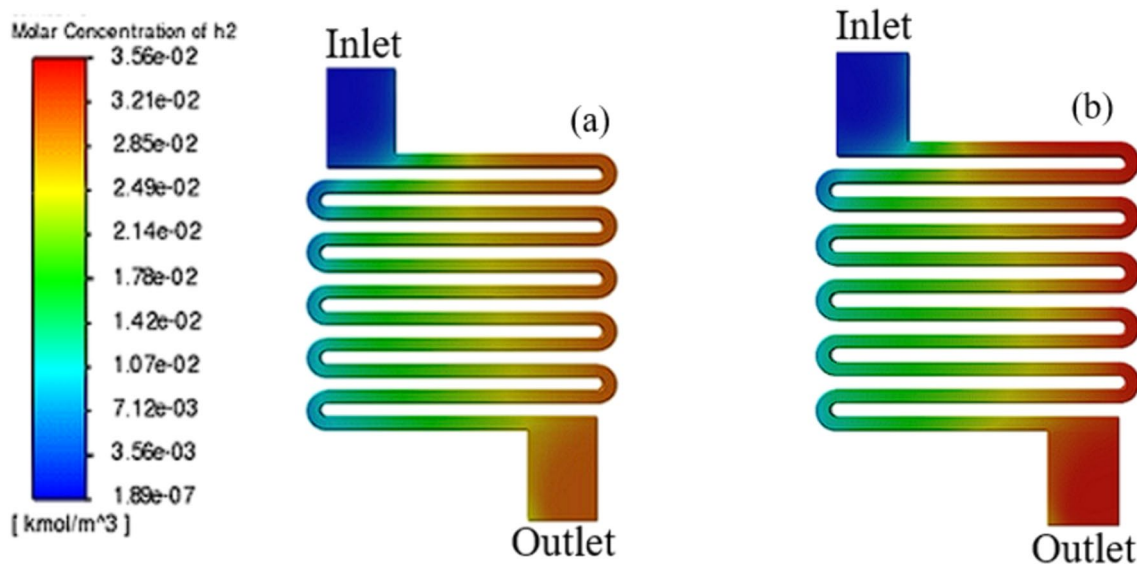
Fig. 6 Concentration (kmol/m^3) of hydrogen at the serpentine cathode channel for simulated voltage levels **a** 1.5 V and **b** 2 V

Fig. 7 Concentration (kmol/m^3) of oxygen at the serpentine anode channel for simulated voltage levels **a** 1.5 V and **b** 2 V
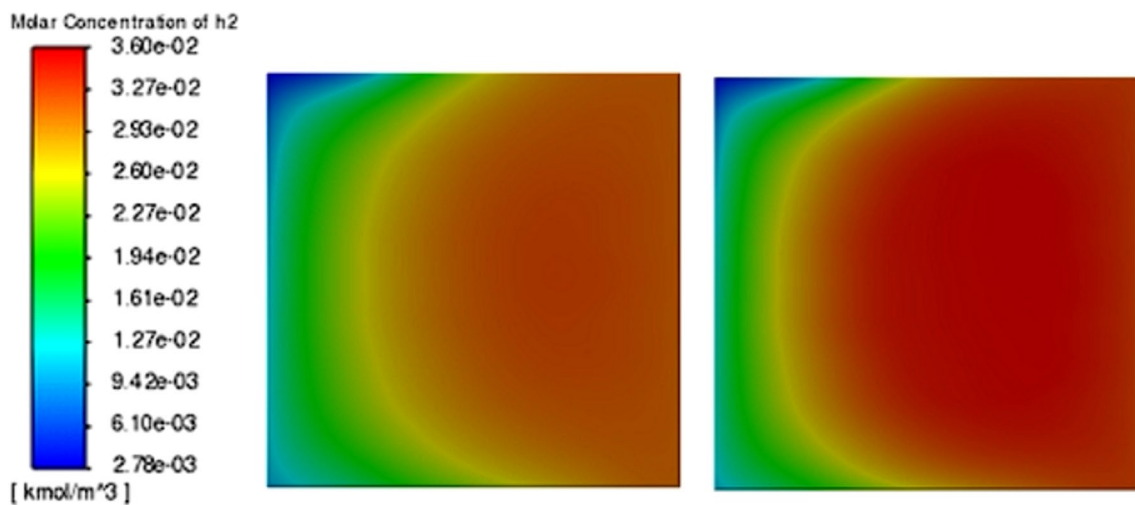
Fig. 8 The concentration (kmol/m^3) of hydrogen at the cathode interface of the membrane for a simulated voltage level of 1.5 V and 2 V

Approximately 700 iterations were conducted to achieve convergence for each set of results, starting from 1.5 V and ending at 2 V, as illustrated in the Figs. 6 and 7, mainly the concentrations of hydrogen and oxygen at the cathode and anode of the PEM electrolyzer's serpentine flow channel, respectively. The findings starting at 1.5 V and 2 V after 1000 iterations are depicted in Figs. 6a, b and 7a, b. With rising voltage, hydrogen and oxygen concentrations rise. The impact of input voltage on the hydrogen content in the serpentine channels is depicted in Fig. 6 a, b. There was

insufficient energy for the electrolyzer to generate enough hydrogen since the temperature set at the electrolyzer's boundary was 343 K.

This is demonstrated in Fig. 7a, where the blue area in the serpentine channel's outflow suggests that no hydrogen is escaping the channel. The bottom part of the channel is where the majority of the hydrogen is produced. The amount of hydrogen produced increases with higher voltage applications and depends on the current flow. The channel is recognized for its winding shape, offering complete coverage for
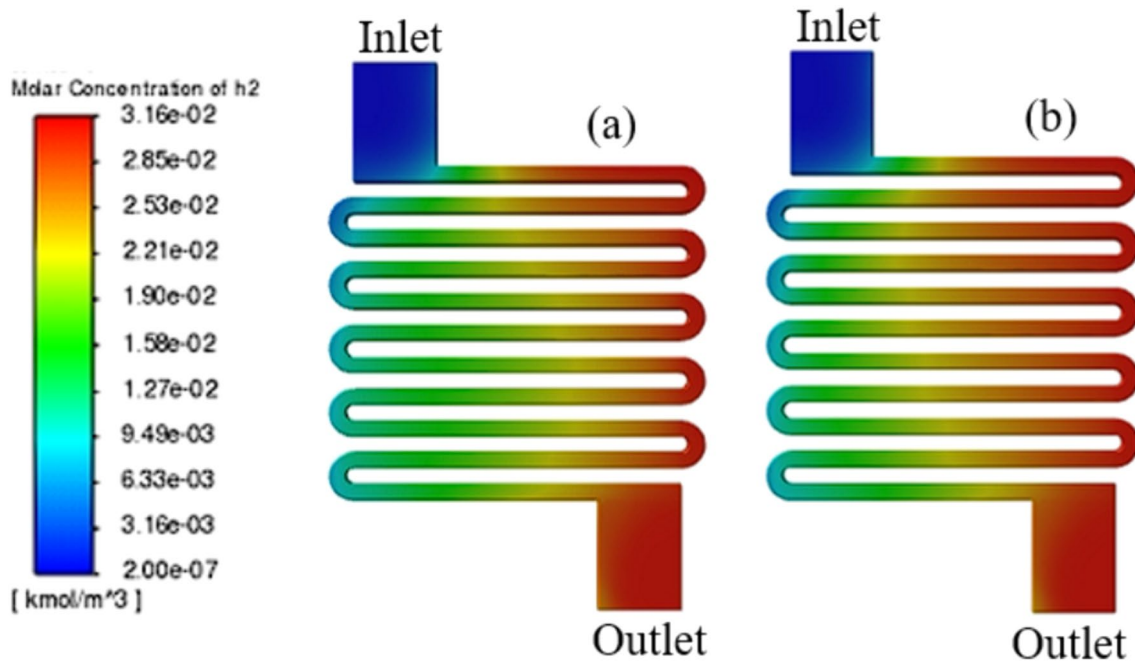
Fig. 9 Concentration (kmol/m³) of hydrogen at the serpentine cathode channel for simulated voltage levels **a** 1.5 V and **b** 2 V
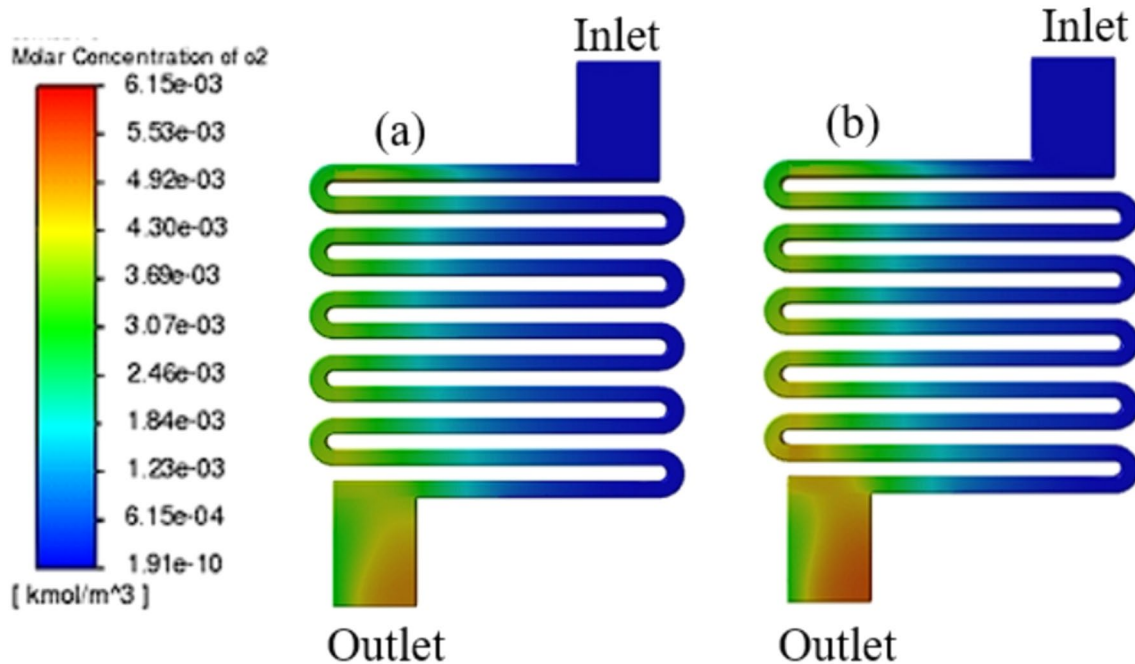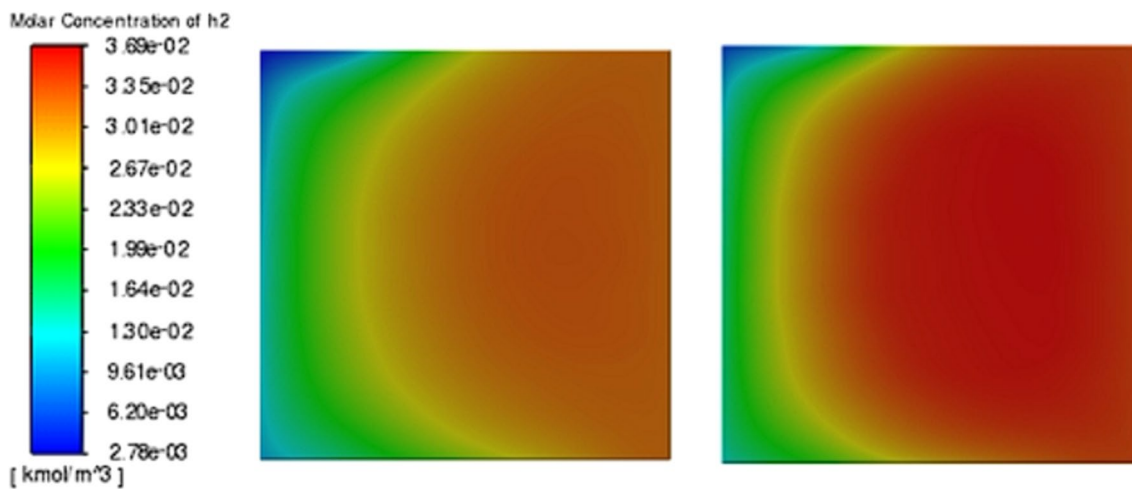

Fig. 10 Concentration (kmol/m³) of oxygen at the serpentine anode channel for simulated voltage levels **a** 1.5 V and **b** 2 V

the reactant at high pressure. However, the winding design leads to reduced performance overall due to losses. The inlet channels have high pressure, which gradually decreases from the entrance to the exit, reflecting the expected pressure drop within the reactant area. With the highest concentration at

the outlet with the SIMPLE scheme, as shown in Fig. 6b at 3.56×10^{-2} kmol/m³, the evolution of the amount of hydrogen at the outflow can be shown to grow. Fig. 7 depicts the concentration of oxygen in the anode outlet side for the two voltages and the maximum reach to 7.07×10^{-3}. The continuous

Fig. 11 Concentration (kmol/m³) of hydrogen at the cathode interface of the membrane for a simulated voltage level of 1.5 V and 2 V

flow plate design guarantees a consistent flow rate. This helps enhance the process by eliminating any excess liquid that may accumulate in the electrolyzer. Water can obstruct the channels by transporting debris to the outlet, hindering gas escape. The constant flow of reactant can block the channel, as shown by the results. Utilizing a serpentine channel in the electrolyzer proves to be efficient.

As illustrated in Fig. 8, the hydrogen concentration at 2 V is higher than at 1.5 V, reaching a value of $3.60\ 10^{-2}$. There is no doubt that the hydrogen and oxygen gases are fleeing the channel based on the distribution of their concentrations.

In the COUPLED scheme, typically, the concentration is highest when the voltage is increased, as displayed in Fig. 9. We can conclude from the Figs. 10 and 11 that the highest recorded hydrogen concentration is $3.69\ 10^{-2}$.

Conclusions

The paper aimed to examine academic literature to assess the current state of CFD modeling of electrolyzers and to simulate a 3D PEM electrolyzer with all relevant physics. Both objectives were successfully achieved. The review of literature revealed variations in modeling approaches among different research papers, primarily due to simplifications such as two-dimensional or isothermal cases. Despite these simplifications, many studies reported successful outcomes and close agreement between simulation results and experimental data. However, it is important to note that the experimental data used for validation mostly consisted of performance data in the form of polarization curves. The CFD simulations performed in the paper involved analyzing heat transfer, turbulence, and electrochemistry, specifically focusing on species and charge transfer. The findings were evaluated against performance data from Majasan et al.

(2021) and were found to align well. The simulation results only differed from the measured data at the lowest voltage levels, a pattern that has been observed in numerous other research studies on the subject. The PEM's performance was demonstrated through contour plots showing hydrogen concentration, revealing that hydrogen production was more pronounced and evenly spread throughout the cell at higher voltages. This was also evident in the high concentration of hydrogen at the outlet on the cathode side. The pressure drops and water velocity have a significant impact on the overall performance of an electrolyzer as they pass through the flow channel. A large pressure drop suggests that there would be less water flowing to the reacting location. As a result, the electrochemical reaction's release of hydrogen will occur at a slower rate. Different sorts of flow channels were taken into consideration to improve the electrolyzer's overall performance. PEM fuel cells were used in the initial experiment as serpentine flow channels. The fuel cell and electrolyzer module in ANSYS Fluent were used to run 3D CFD simulations to examine the impact of serpentine flow channels on the performance of PEM electrolyzers. It was discovered that the serpentine flow channels had the highest oxygen and hydrogen concentrations, between 1.5 V and 2 V. Maximum hydrogen concentration in serpentine flow channels at steady conditions is $3.56\ 10^{-2}$ kmol/m³.

The current approach would greatly benefit from more measurements, including the total mass concentration of hydrogen on the cathode side, as well as monitoring temperatures and pressure levels within the PEM. Of the two pressure–velocity coupling methods used, the SIMPLE scheme provided a simpler simulation process and quicker convergence times, but it did not allow for turbulence modeling. In contrast, the COUPLED scheme offered more stable and robust convergence and the ability to model turbulence, although it required more computational time and a less

automated simulation process. The COUPLED scheme also requires more complex initialization methods compared with the SIMPLE scheme. Despite its drawbacks, the COUPLED pressure–velocity coupling method is still recommended for future simulations as the preferred choice.

Declarations

Conflicts of interest The authors declare no conflict of interest.

References

Baaloudj O et al. (2022) Bismuth Sillenite crystals as recent photocatalysts for water treatment and energy generation: a critical review. Catalysts. https://doi.org/10.3390/catal12050500

Carmo M, Fritz DL, Mergel J, Stolten D (2013) A comprehensive review on PEM water electrolysis. Int J Hydrogen Energy 38(12):4901–4934. https://doi.org/10.1016/j.ijhydene.2013.01.151

de Sousa JVN et al. (2020) On the study of autonomous underwater vehicles by computational fluid-dynamics. Open J Fluid Dyn. https://doi.org/10.4236/ojfd.2020.101005

Grigoriev SA, Fateev VN, Bessarabov DG, Millet P (2020) Current status, research trends, and challenges in water electrolysis science and technology. Int J Hydrogen Energy 45(49):26036–26058. https://doi.org/10.1016/j.ijhydene.2020.03.109

Ijaodola OS et al. (2019) Energy efficiency improvements by investigating the water flooding management on proton exchange membrane fuel cell (PEMFC). Energy 179:246–267. https://doi.org/10.1016/j.energy.2019.04.074

Jouhara H, Żabnieńska-Góra A, Khordehgah N, Ahmad D, Lipinski T (2020a) Latent thermal energy storage technologies and applications: a review. Int J Thermofluids. https://doi.org/10.1016/j.ijft.2020.100039

Jouhara H, Serey N, Khordehgah N, Bennett R, Almahmoud S, Lester SP (2020b) Investigation, development and experimental analyses of a heat pipe based battery thermal management system. Int J Thermofluids 1–2:100004. https://doi.org/10.1016/j.ijft.2019.100004

Kenfoud H, Nasrallah N, Baaloudj O, Belabed C, Chaabane T, Trari M (2022) Opto-electrochemical characteristics of synthesized BaFe2O4 nanocomposites: photocatalytic degradation and hydrogen generation investigation. Int J Hydrogen Energy. https://doi.org/10.1016/j.ijhydene.2022.01.232

Khatib FN, Wilberforce T, Thompson J, Olabi AG (2021) Experimental and analytical study of open pore cellular foam material on the performance of proton exchange membrane electrolysers. Int J Thermofluids 9:100068. https://doi.org/10.1016/j.ijft.2021.100068

Lu X et al. (2023) Optimization of power allocation for wind-hydrogen system multi-stack PEM water electrolyzer considering degradation conditions. Int J Hydrogen Energy 48(15):5850–5872. https://doi.org/10.1016/J.IJHYDENE.2022.11.092

Ma Z, Witteman L, Wrubel JA, Bender G (2021) A comprehensive modeling method for proton exchange membrane electrolyzer development. Int J Hydrogen Energy 46(34):17627–17643. https://doi.org/10.1016/j.ijhydene.2021.02.170

Majasan JO, Cho JIS, Maier M, Shearing PR, Brett DJL (2021) Optimisation of mass transport parameters in a polymer electrolyte membrane electrolyser using factorial design-of-experiment. Front Energy Res 9(April):1–9. https://doi.org/10.3389/fenrg.2021.643587

Ni A, Upadhyay M, Kumar SS, Uwitonze H, Lim H (2023) Anode analysis and modelling hydrodynamic behaviour of the multiphase flow field in circular PEM water electrolyzer. Int J Hydrogen Energy 48(43):16176–16183. https://doi.org/10.1016/j.ijhydene.2023.01.032

Ozdemir SN, Taymaz I, San FGB, Okumuş E (2024) Performance assessment and optimization of the PEM water electrolyzer by coupled response surface methodology and finite element modeling. Fuel. https://doi.org/10.1016/j.fuel.2024.131138

Shiva Kumar S, Himabindu V (2019) Hydrogen production by PEM water electrolysis—A review. Mater Sci Energy Technol 2(3):442–454. https://doi.org/10.1016/j.mset.2019.03.002

Wang C, Feng L (2023) Recent advances and perspectives of Ir-based anode catalysts in PEM water electrolysis. Energy Adv 3(1):14–29. https://doi.org/10.1039/d3ya00492a

Wilberforce T, Khatib FN, Ogungbemi E, Olabi AG (2018) Water electrolysis technology. Ref Modul Mater Sci Mater Eng. https://doi.org/10.1016/b978-0-12-803581-8.11273-1

Wu X, Tayal J, Basu S, Scott K (2011) Nano-crystalline RuxSn1—XO2 powder catalysts for oxygen evolution reaction in proton exchange membrane water electrolysers. Int J Hydrogen Energy 36(22):14796–14804. https://doi.org/10.1016/j.ijhydene.2011.01.067